

https://dspace.org/

The ultrastructure and taxonomy of protosinphon botryoides (Kutz) Klebs

Birkhead, Monica

2015-01-09
http://hdl.handle.net/10539/16297

Downloaded from a DSpace repository. https://dspace.org/

Figure 73. A chloroplast portion in which the intergranal thylakoids are no longer apparent, thereby separating the pseudograna from one another. (Scale = 0.5μm).

Figure 74. An isolated pseudogranum enclosed by a hemimembrane with attached lipocarotenoids. (Scale = 1μm).

Figure 75. Numerous isolated chloroplast portions (pseudograna) are associated with irregular lipocarotenoid material that is continuous with the linear arrays lining the wall. (Scale = 2μm).

Figure 76. A small chloroplast remnant surrounded by concentric arrays of lipocarotenoid-studded hemimembranes (arrowheads), the innermost of which is the chloroplast's outer membrane (arrows). (Scale = 1μm)

Figure 77. The thylakoids and pseudograna of the chloroplast profile have become convoluted and expanded in a manner reminiscent of many other green algal resting cells. (Scale = 0.5μm).

Figure 78. A degenerating chloroplast with a chaotic maze of contorted thylakoids, and surrounded by lipocarotenoid material (Scale = 1μm).


79
Ql
pg
C
80
Ql
S
81
S
pg
82
S
k1
Ql

Figure 79. The initation of a thylakoid plexus within a membrane enclosing pseudograna (Scale = 0.5µm).

Figure 80. A thylakoid plexus with an extension (arrowheads) enclosing a starch grain. (Scale = 0.5µm).

Figure 81. A developing plexus with both starch and pseudogranal thylakoid associations (arrowheads). (Scale = 1µm).

Figure 82. Lipid droplets (arrowheads) occurring within the same vesicle as a type 1 crystal, and the lipocarotenoid material from which both lipid and crystal are derived (Scale = 0.3µm).

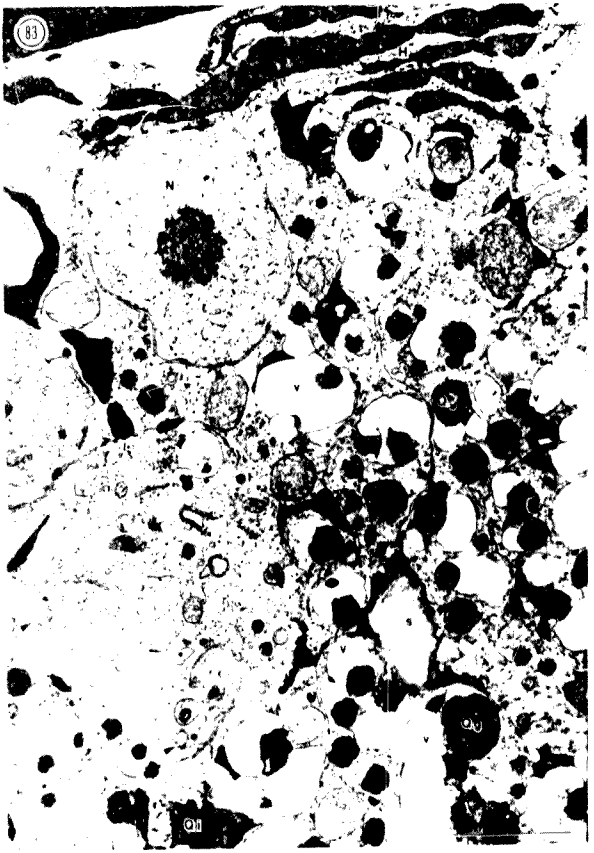
83
H
N
V
V
V
V
Q1

Figure 83. A coenocyst five hours after zoosporogenic induction. Endomembrane proliferation is evident, especially in the number of annular cisternae (arrowheads) that resemble an initial stage in Golgi replication. Lipocarotenoid digestion has left numerous empty vesicles (more numerous than in inactive coenocysts). (Scale = 1μm).


84
85
87
86
88

Figure 84. A regreening coenocyst with a newly formed pyrenoid and actively elongating intergranal thylakoids (arrowheads) which connect the previously isolated pseudograna. (Scale = 1μm).

Figure 85. Small tubules (arrowheads) occur in the chloroplast matrix subtended by young thylakoids. (Scale = 2.5μm).

Figure 86. A partially regreened coenocyst contains chloroplasts with tubular elements (arrowheads). (Scale = 2μm).

Figure 87. The endomembrane system of regreening coenocysts proliferates and the dictyosomes increase in number, often being paired across a nucleus. (Scale = 1μm).

Figure 88. Golgi replication may occur by the formation of annular cisternae, which are then released and unfurl to form the first cisterna in a dictyosomal stack. (Scale = 0.25μm).


89
D
N
D
90
P
S
91
B
N
D
92
D
N
B
93
CF
QN

Figure 89. A second method of Golgi replication involves vertical cleavage through a dictyosomal stack. (Scale = 0.25μm).

Figure 90. During zoosporogenesis, pyrenoids are lost - a process initiated by loss of the starch sheath and intermingling of the pyrenoid and chloroplast thylakoids. (Scale = 5μm).

Figure 91. The initial stage in basal body formation where the developing basal bodies lie at 90° to the dictyosome. (Scale = 0.5μm)

Figure 92. A later stage of zoosporogenesis in which basal body rotation has occurred so that the basal bodies and dictyosome are in a line. (Scale = 0.5μm).

Figure 93. Cleavage furrows appear as two compressed membranes (arrowheads) which then separate, with the resultant furrow often filled with substances such as lipocarotenoids. (Scale = 1.5μm).

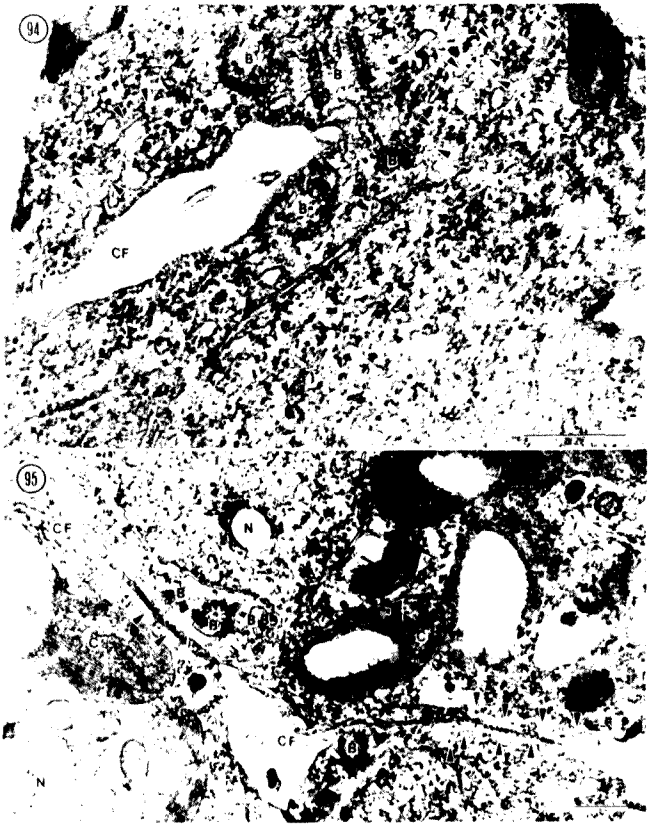
94
B
B
B
B
CF
95
CF
N
B
B
CF
B
N

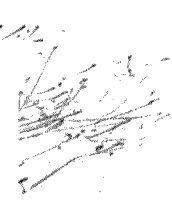

Figure 94. Paired basal bodies apposed across a developing furrow that is lined by microtubular arrays (arrowheads). (Scale = 0.25μm).

Figure 95. Microtubules (arrowheads) lie along the paths of the cleavage furrows. (Scale = 0.25μm).

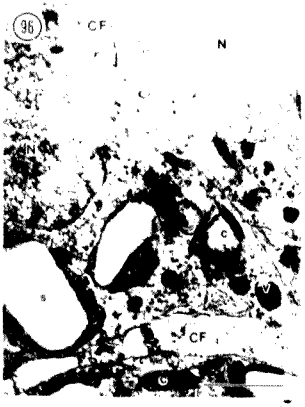
96
CF
N
C
CF
C


97


98
W


99

Figure 96. Cleavage furrows, filled with membranous inclusions, extending between developing zoospores. (Scale = 1µm).

Figure 97. Two coenocysts still enclosed within a parental wall, which are dividing to form zoospores. Arrowheads indicate some of the numerous furrows that are dividing the cytoplasm. (Scale = 5µm).

Figure 98. Zoospores, some of which are not fully separated from each other, enclosed within the parent wall. (Scale = 2µm).

Figure 99. Cross-section through a young siphon that has produced zoospores which will be released via the thinned wall region (arrowheads). (Scale = 8µm).

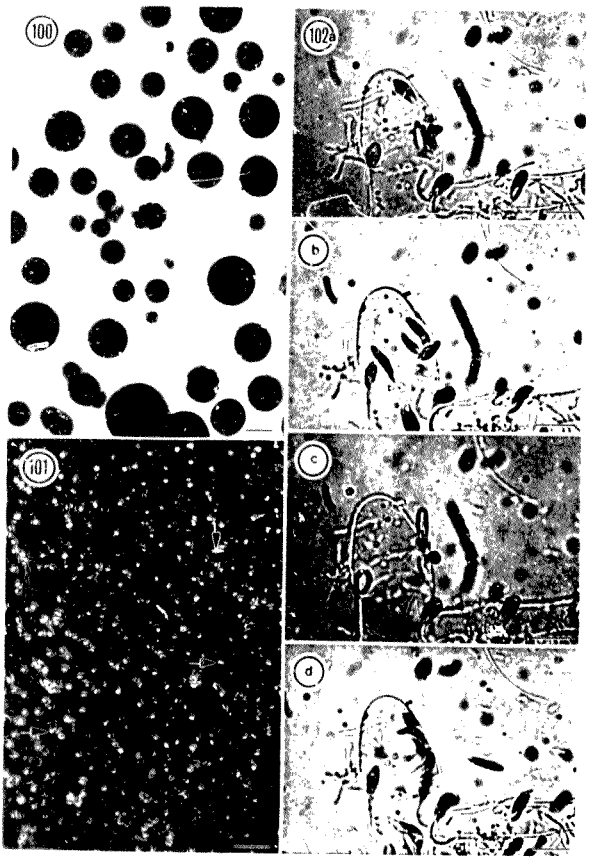
100
101
102a
b
c
d

Figure 100. Coenocysts undergoing zoosporogenesis. (Scale = 22μm).

Figure 101. Zoospores (phase contrast). Note the cells joined posteriorly (arrows). (Scale = 25μm).

Figure 102a-d. A sequence of zoospore escape via a parental wall pore. (Scale = 8.5μm).

(103)



(104)



(105)



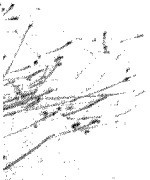

Figure 103. The numerous empty walls left after successful zoospore release. Note the zygotes (!) and the cysts still undergoing zoosporogenesis. (Scale = 30µm).

Figure 104. Zoospores of various shapes. (Scale = 10µm).

Figure 105. Zoospores approaching, and adhering to, the floating mat formed by hundreds of settled cells. (Scale = 20µm).

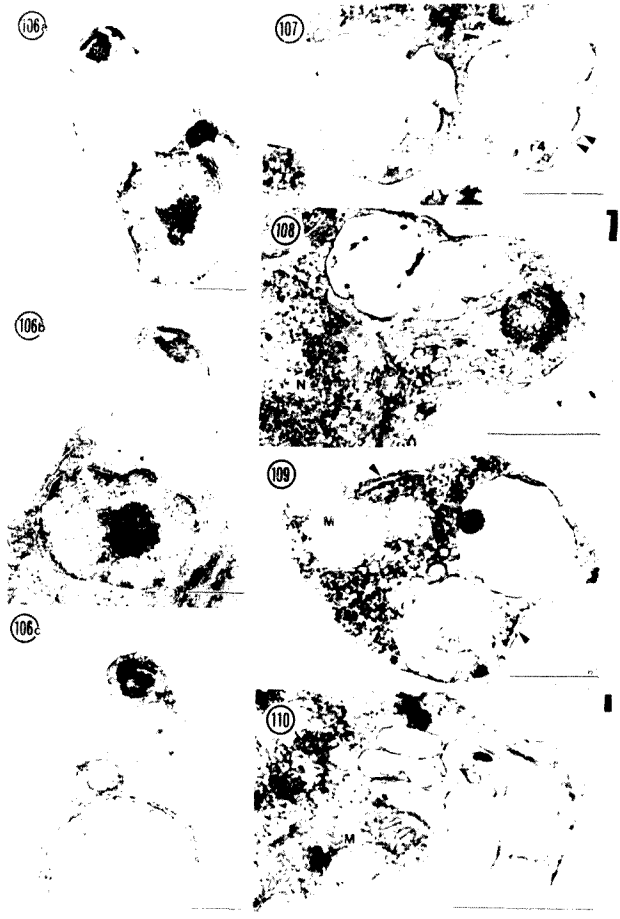
106a
106b
106c
107
108
N
109
M
110
M

Figure 106a-c. A series of longitudinal sections perpindicular to the plane of flagellar insertion (TLS), through the zoospore apex. The sequence is of contractile vacuole bursting : 106a - fully extended; 106b - time of rupture; 106c - erupted, with the adjacent vacuole intact. (Scale = 0.5µm).

Figure 107. Cross-section through zoospore apex in the region of the contractile vacuoles, which are fully dilated. The vacuoles are supported by the microtubular roots and the cytoskeletal microtubules (arrowheads). (Scale = 0.5µm).

Figure 108. TLS of zoospore with one distended contractile vacuole containing waste material, and one contractile vacuole forming by vesicle coalescence. (Scale = 0.5µm).

Figure 109. Tangential cross-section of zoospore apex with one fully formed contractile vacuole, and one vacuole filled with vesicular material collected during vacuolar formation. ER profiles line the contractile vacuoles (arrowheads). (Scale = 0.5µm).

Figure 110. Tangential BLS (longitudinal section in the plane of the flagellar insertion) of a zoospore apex showing aggregation and fusion of membrane-filled vacuolar vesicles. (Scale = 0.5µm).


111
114
112
113

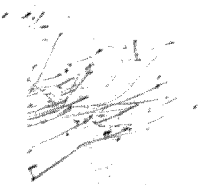

Figure 111. TLS of zoospore apex with mitochondrial profile cupping the forming contractile vacuole. (Scale = 0.5µm).

Figure 112. TLS of zoospore with nuclear projection towards basal body (arrowheads). (Scale = 0.5µm).

Figure 113. BLS of zoospore showing nuclear concavity below contractile vacuole (between arrowheads). (Scale = 0.5µm).

Figure 114. Tangential cross-section revealing nuclear concavity filled with cytoplasm above which a contractile vacuole rests (arrowhead), and the narrow median ridge (arrow) which lies between the two contractile vacuoles. (Scale = 1µm).


115
C
M
U
116
117
U
D
118
D
119
V
D



Figure 115. Central portion of a zoospore, with a pored nucleus associated with the dictyosomal forming face, and a microbody and a mitochondrial profile adpressed to the outer nuclear membrane. (Scale = 0.5µm).

Figure 116. TLS of a typical zoospore with central and posterior vesicles, lobed chloroplast, and peripheral ER (arrowheads). (Scale = 0.5µm).

Figure 117. An infrequent arrangement of two dictyosomes lying below a zoospore nucleus. (Scale = 0.5µm).

Figure 118. A longitudinally sectioned zoospore containing an unusually long, sinuous dictyosome. (Scale = 0.5µm).

Figure 119. The posterior portion of a zoospore, lined with ER, and filled with vesicles and lipid. The chloroplast lobe contains an incipient pyrenoid embedded in chloroplast stroma. (Scale = 0.5µm).

(120)



(121)



(122)

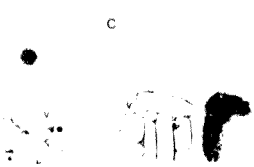

(123)



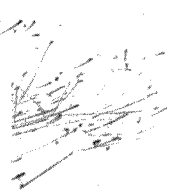

Figure 120. Extensive mitochondrial profiles occurring anteriorly in a vesicle-filled zoospore. (*Scale = 1µm*).

Figure 121. The eyespot is embedded in the anterior chloroplast lobe, and the nucleus is framed by mitochondrial cisternae and two microbodies. Vesicles occur centrally and posteriorly. (Scale = 1µm).

Figure 122. The posterior region of a zoospore containing crystals and lipid. (Scale = 0.5µm).

Figure 123. A zoospore BLS showing extensive lipocarotenoid accumulations centrally, and particularly posteriorly. The cup-shaped chloroplast holds a central pyrenoid. (Scale = 1µm).


124
126
124
127
125
128
129

Figure 124. A TLS of a zoospore with a chloroplast lobe extending beyond the nucleus, and containing the uniseriate eyespot. (Scale = 0.5μm). INSET: a tangential section of an eyespot showing the hexagonal packing of the constituent globules. (Scale = 0.2μm).

Figure 125. A zoospore containing two pyrenoids, peripherally situated in the cup-shaped chloroplast. (Scale = 0.5μm).

Figures 126-129. A pyrenoid developmental series in zoospores - from a pyrenoid matrix with few intrapyrenoidal thylakoids and some associated chloroplast tubules (arrowheads) - Figure 126; to a matrix subtended by a number of elongate thylakoids - Figure 127; to the beginnings of the starch sheath formation - Figure 128; and finally the complete pyrenoid sheath - Figure 129. (Scales = 0.5μm).


130
131
M
M
132
133

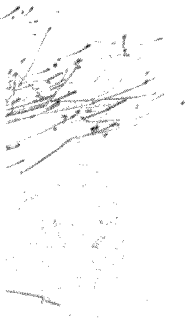

Figure 130. A tangentially sectioned zoospore with an extensive mitochondrial profile posteriorly, and an RER fragment (arrowhead). (Scale = 1µm).

Figure 131. The large mitochondrial profile that curves upwards past the nucleus to the base of the contractile vacuoles, in the zoospores. (Scale = 0.5µm).

Figure 132. The two-stranded hairpoint of the zoospore, formed by the extension of the central microtubule pair (arrowhead). (Scale = 0.5µm).

Figure 133. A negatively-stained flagellum in which both the A-tubule termination (arrowheads) and the helical gyres of the central microtubule pair cap (arrows) are apparent. (Scale = 0.5µm).

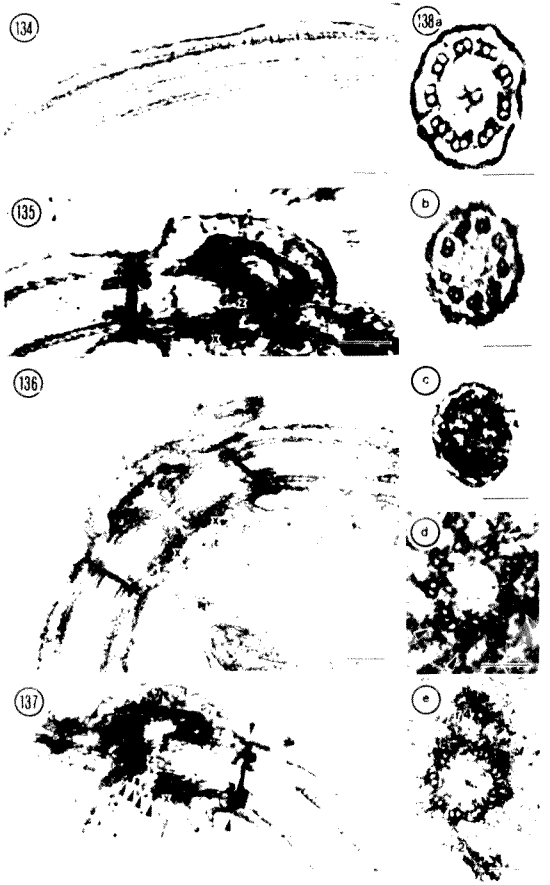
134
138a
135
b
136
c
d
137
e

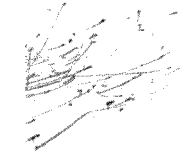

Figure 134. A longitudinally sectioned zoospore flagellum in which the paired secondary fibres (arrows) are clearly visible. (Scale = 0.1µm).

Figure 135. A tangential BLS through the flagellar apparatus, showing the distinct transition region and basal body ultrastructure. (Scale = 0.1µm).

Figure 136. A zoospore in which the two subunits of the proximal sheath are not joined, and in which the two transition regions are well-defined. Note the hairpoint lying above the zoospore apex. (Scale = 0.1µm).

Figure 137. Extensions occur from the septum of the transition region to the flagellar membrane (arrows). The striations of a proximal band (arrowheads) can be seen to extend from the proximal sheath of one basal body across to the other basal body. (Scale = 0.1µm).

Figure 138a-e. A series of cross-sections through the flagellum. Axoneme (a); stellate pattern of the transition region (b); septum of the transition region (c), the juncture of transition region and basal body (d), transition fibres (arrowheads) extending outwards from the microtubules; the triplet pattern of the basal body (e). (Scale = 0.1µm).


139
B1
B2
140
B1
B2
141
142
B1
B2
143
144

Figure 139. Flagellar apparatus as viewed from the anterior end of the *zoospore*, displaying clockwise basal body rotation, connectives between each basal body and a 2-stranded microtubular root (arrowheads), and proximal fibres extending between the basal bodies (arrows). (Scale = 0.1µm).

Figure 140. Anterior view of cross-sectioned basal bodies connected by proximal fibres (arrowheads). (Scale = 0.1µm).

Figure 141. Cross-section of a basal body in the cartwheel region, with the R2 and associated electron dense material and SMAC curving over the basal body. The trilobed proximal sheath (arrowheads) underlies the three most posterior triplets. Both microtubular roots are connected to the basal body by electron dense material. (Scale = 0.1µm).

Figure 142. Basal body orientation viewed from the anterior end of a *zoospore*. One proximal fibre is evident (arrowhead), as is the electron dense material to which the R4s attach to the basal bodies. (Scale = 0.1µm)

Figure 143. A BLS in which the distal striated fibre is attached to both the triplet and the cartwheel regions of each basal body. (Scale = 0.1µm).

Figure 144. Grazing section of a distal striated fibre showing the cross-striations and perpendicularly-aligned constituent fibres. (Scale = 0.1µm).

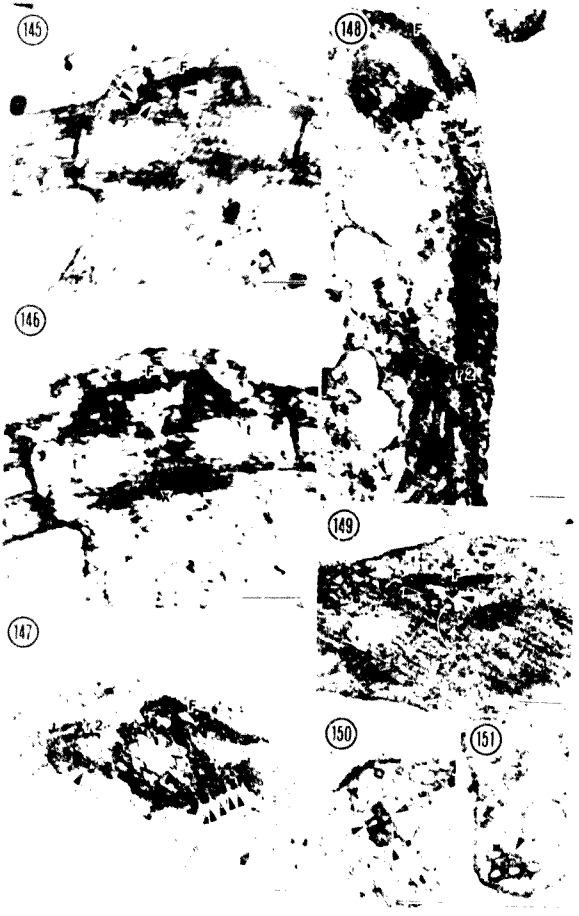
145
146
147
148
149
150
151

Figure 145. A BLS showing the fibres composing the attachment arms of the distal striated fibre (arrows). The small connectives between the distal fibre and the microtubules of the R2 (arrowheads), appear to form one of the distal fibre-basal body connections. (Scale = 0.1µm).

Figure 146. A rare section in which the two subunits of the proximal sheath are continuous along the lower surfaces of the basal bodies. The ends of the proximal sheath terminate in the triplet region. (Scale = 0.1µm).

Figure 147. A tangentially sectioned basal body illustrating the basal body-R2 connection, and the striated proximal fibre (arrowheads). (Scale = 0.1um).

Figure 148. A tangential section through an R2, which reveals the associated electro material and SMAC (arrowheads). (Scale = 0.1µm).

Figure 149. TL tangential section showing the small connectives (arrowheads) between the distal fibre and the R2 microtubules. (Scale = 0.1µm).

Figure 150. A cross-section through the R2 microtubules (arrows) and the associated SMAC (arrowhead). Note the cytoskeletal microtubules, and the electron dense material associated with the R2. (Scale = 0.1µm).

Figure 151. The three-over-one microtubular arrangement of the R4 with its associated electron dense material (arrowhead). (Scale = 0.1µm).


152
155
153
156
154

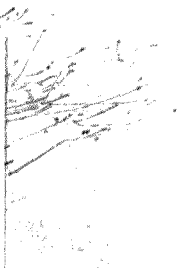

Figure 152. Newly settled zoospores with an active dictyosome producing vesicles filled with wall material (arrowheads). The chloroplast thylakoids are elongate and pseudograna1 formation is just beginning. (Scale = 1µm).

Figure 153. An active dictyosome producing vesicles filled with fibrils of wall material. (Scale = 0.1µm).

Figure 154. A settled zoospore with a thick wall. The discontinuity between wall and *plasmalemma* contains membranous fragments (arrowheads). (Scale = 0.5µm).

Figure 155. A resorped flagellar axoneme lies inside the plasmalemma. (Scale = 0.5µm).

Figure 156. The wall fibres of two settled zoospores intermingle and cause the zoospores to adhere to one another. Small vesicles filled with wall material (arrowheads) can be seen lining the plasmalemma. (Scale = 0.25µm).

Author Birkhead Monica
Name of thesis The Ultrastructure And Taxonomy Of Protosiphon Botryoides (kutz) Klebs. 1988

PUBLISHER:
University of the Witwatersrand, Johannesburg
©2013

LEGAL NOTICES:

Copyright Notice: All materials on the University of the Witwatersrand, Johannesburg Library website are protected by South African copyright law and may not be distributed, transmitted, displayed, or otherwise published in any format, without the prior written permission of the copyright owner.

Disclaimer and Terms of Use: Provided that you maintain all copyright and other notices contained therein, you may download material (one machine readable copy and one print copy per page) for your personal and/or educational non-commercial use only.

The University of the Witwatersrand, Johannesburg, is not responsible for any errors or omissions and excludes any and all liability for any errors in or omissions from the information on the Library website.